



Physics of Coupled, Multi-Scale Nonequilibrium Flows

D. A. Levin* and V. Patil*

Sergey G. Gimelshein**

Joanna M. Austin***

****Department of Aerospace Engineering***

The Pennsylvania State University, University Park, PA 16802

***** University of Southern California, Los Angeles, CA 90089***

******University of Illinois, Urbana-Champaign, IL 61801***

AFOSR Aerothermodynamics Reviews

July 15-18, 2013

AFOSR BRICC

Research Motivation

- Hypersonic flows are characterized by spatial regions with both sub and supersonic flow in various degrees of thermochemical non-equilibrium and multiple length scales..
- Navier-Stokes (NS) based continuum techniques encounter physical challenges in rarefied regions and are unable to capture the non-equilibrium phenomena.
- An accurate modeling of such flows requires a kinetic consideration.
- Kinetic methods, such as DSMC, are accurate but can be expensive, especially when applied to high density, low Kn flows.
- DSMC is a relatively mature approach to solving the Boltzmann equ.

What's new?





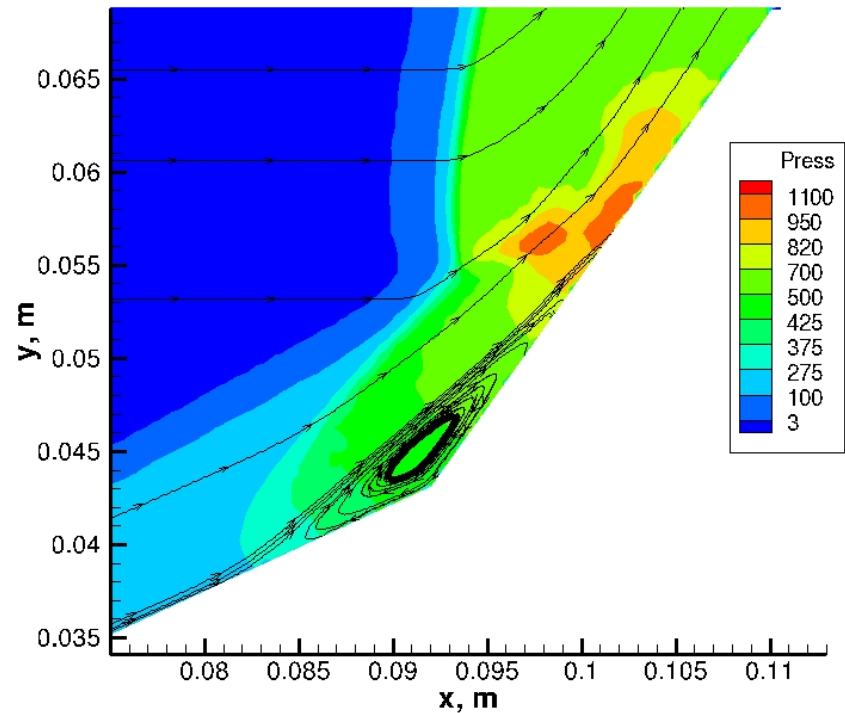
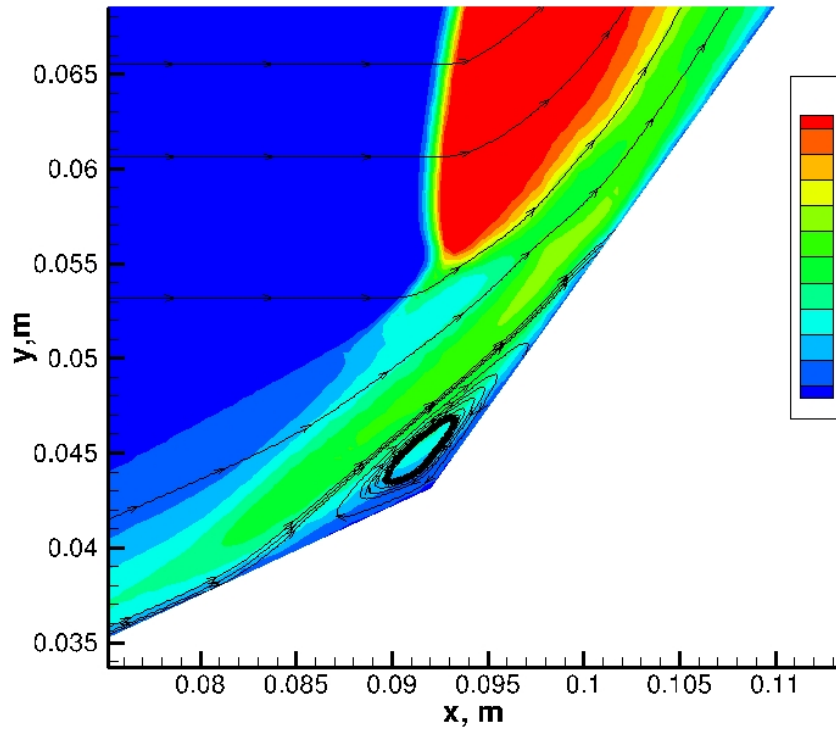
(1) Double Cone Studies of Moss and Bird*

Experimental conditions performed for Mach 15.6 nitrogen flow about a 25-/55-deg bi-conic model

| Freestream Parameters : | |
|-------------------------|------------------------|
| Temperature, K | 42.6 |
| Number Density, m^3 | 3.779×10^{21} |
| Speed, m/s | 2073 |
| Density, kg/m^3 | 1.757×10^{-4} |
| Pressure, Pa | 2.23 |
| Mach number | 15.6 |
| Reynolds number | 1.37467×10^5 |
| Knudsen number | 1.7×10^{-4} |

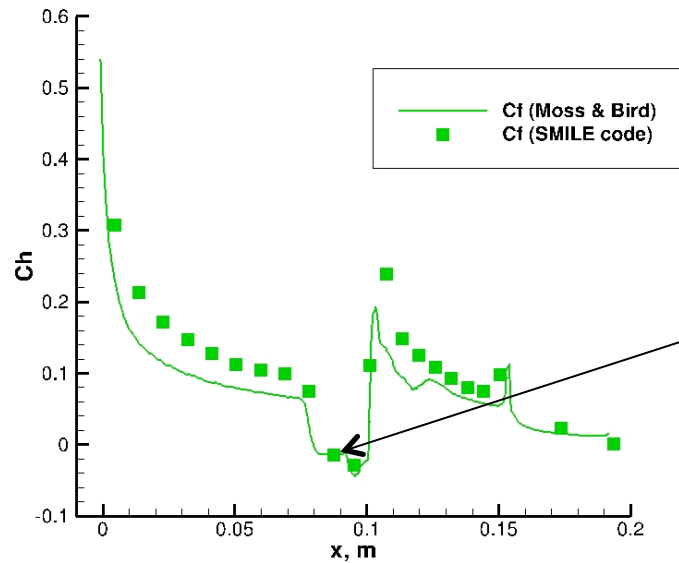
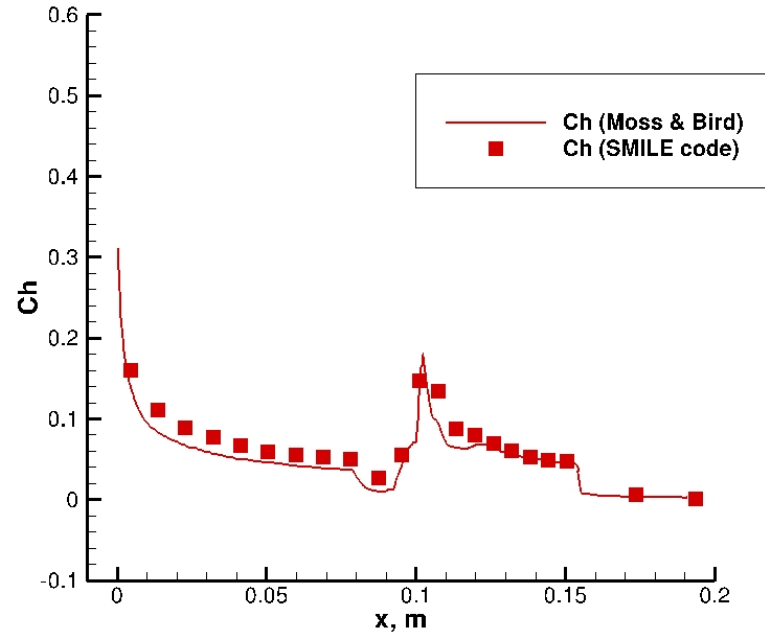
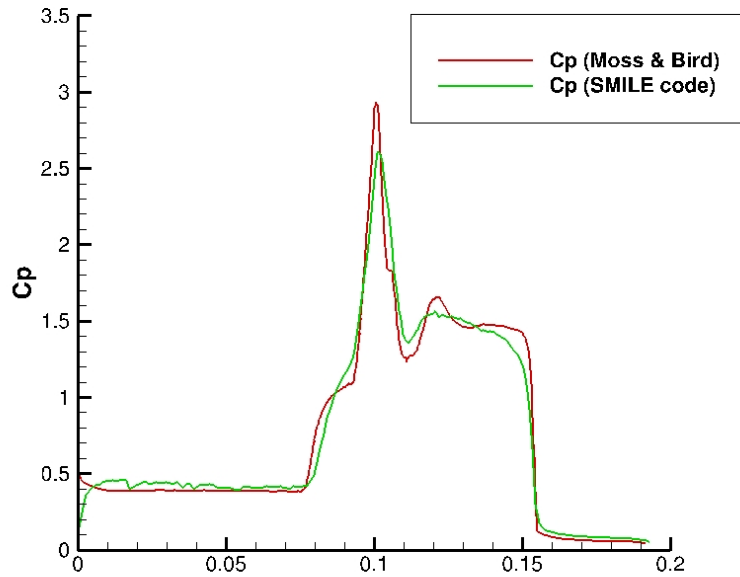
*Moss, J. N. and Bird, G. A., "Direct Simulation Monte Carlo of Hypersonic Flows with Shock Interactions," *AIAA Journal*, Vol. 43, No. 12, 2005, pp. 2565-2573.

Double Cone Temperature and Pressure Contours



- Physics is dominated by presence of separation zone and
- Sharp leading edge.

Comparison of Surface Profiles – Double Cone Configuration



- Separation zone well modeled.

(2) HET Mach 7 Nitrogen Flows

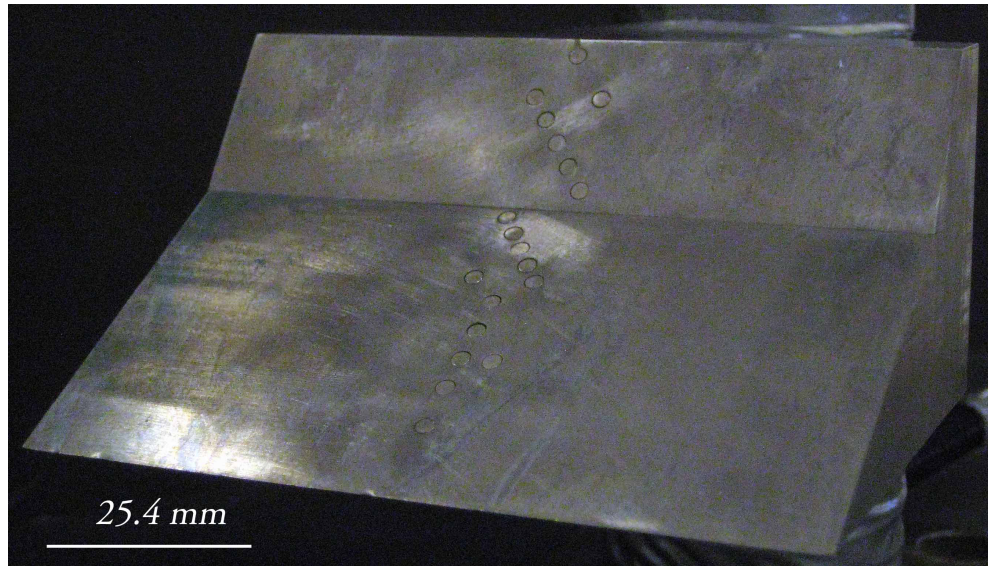


Figure 2. The experimental double wedge model used in the current study. The coaxial thermocouple gauges can be seen along the center of the model. Note: Some gauges are staggered to increase spatial resolution.

- **Computational study of the complex shock interactions resulting from the hypersonic flow about a double wedge configuration presented in the paper AIAA 2012-0284 by A.B. Swantek and J. M. Austin.**
- **Stagnation enthalpies from 2-8 MJ/kg, about a 30-/55-deg double wedge model.**



Summary of 2 HET Freestream Conditions

| Freestream Parameters | M 7_8 (High Enthalpy) | M 7_2 (Low Enthalpy) |
|---------------------------------|--------------------------|-------------------------|
| Mach number | 7.14 | 7.11 |
| Static Temperature, K | 710 | 191 |
| Static Pressure, kPA | 0.78 | 0.39 |
| Velocity, m/s | 3812 | 1972 |
| Density, kg/m ³ | 0.0037 | 0.0069 |
| Number Density, /m ³ | 7.96×10^{22} | 1.48×10^{23} |
| Stagnation Enthalpy, MJ/kg | 8.0 | 2.1 |
| Unit Reynolds number, /m | 0.4156×10^6 | 1.0653×10^6 |
| Knudsen number | 4.0256×10^{-4} | 1.5742×10^{-4} |

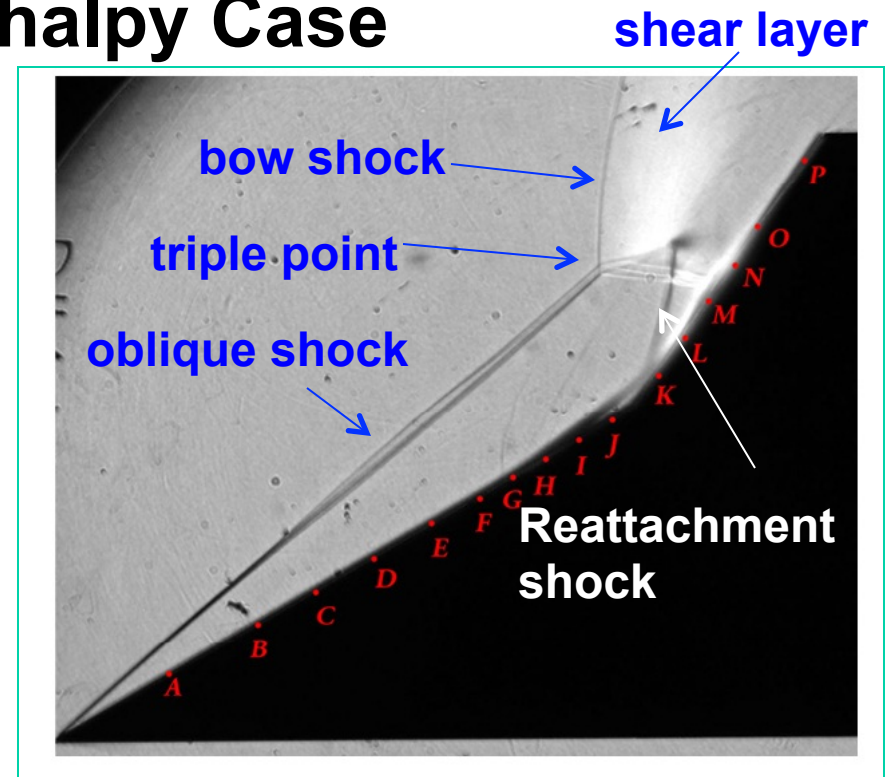
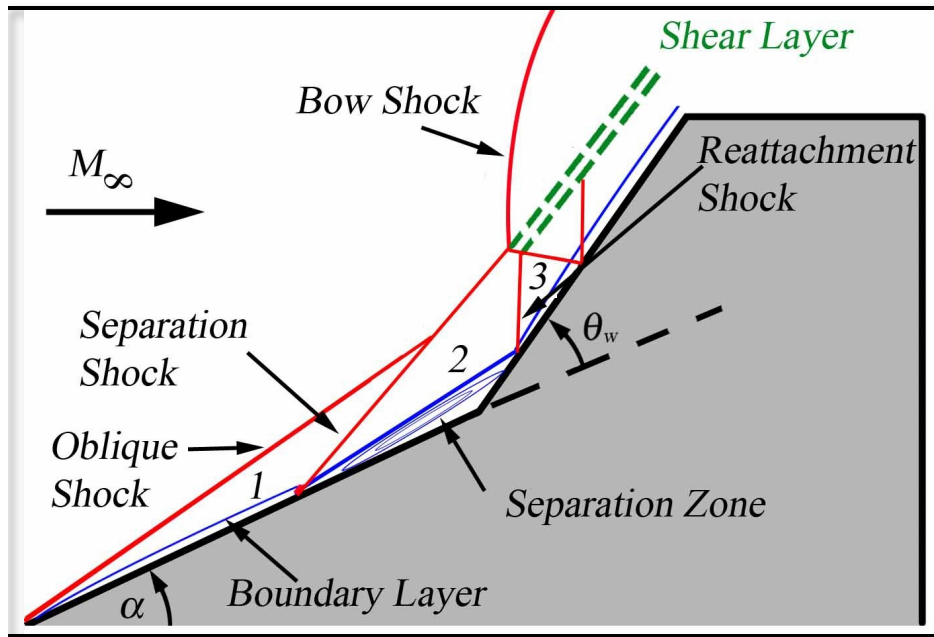
Convergence of Solution*

- Total number of simulated particles = 9.8×10^7
 Number of particles per cell = > 30
 Number of particles per λ^2 = 3 to 4
 Therefore, sufficient number of particles present in domain.
- Local Knudsen number ($Kn = \lambda/L$) –
 Local Kn values > 0.1 everywhere in domain.
 Therefore, cell size of sufficient order.
- Mean time between collisions > Timestep
- So, we can conclude that the solution is converged.

| Numerical Parameters | M 7_8 (High Enthalpy) |
|---|-----------------------|
| Total number of time-steps (NSTEP) | 100,000 |
| Time step (TAU), s | 1.0×10^{-9} |
| Number of molecules in one simulated particle (PFnum) | 1.0×10^{13} |
| Number of cells | 450 x 400 |
| Cell size, m | 2.0×10^{-4} |
| Grid Adaptation (NPG) | 20 |
| Number of processors | 64 |

***Many thanks to Dr. Ryan Gosse for providing assistance with the Air Force HPC Machines.**

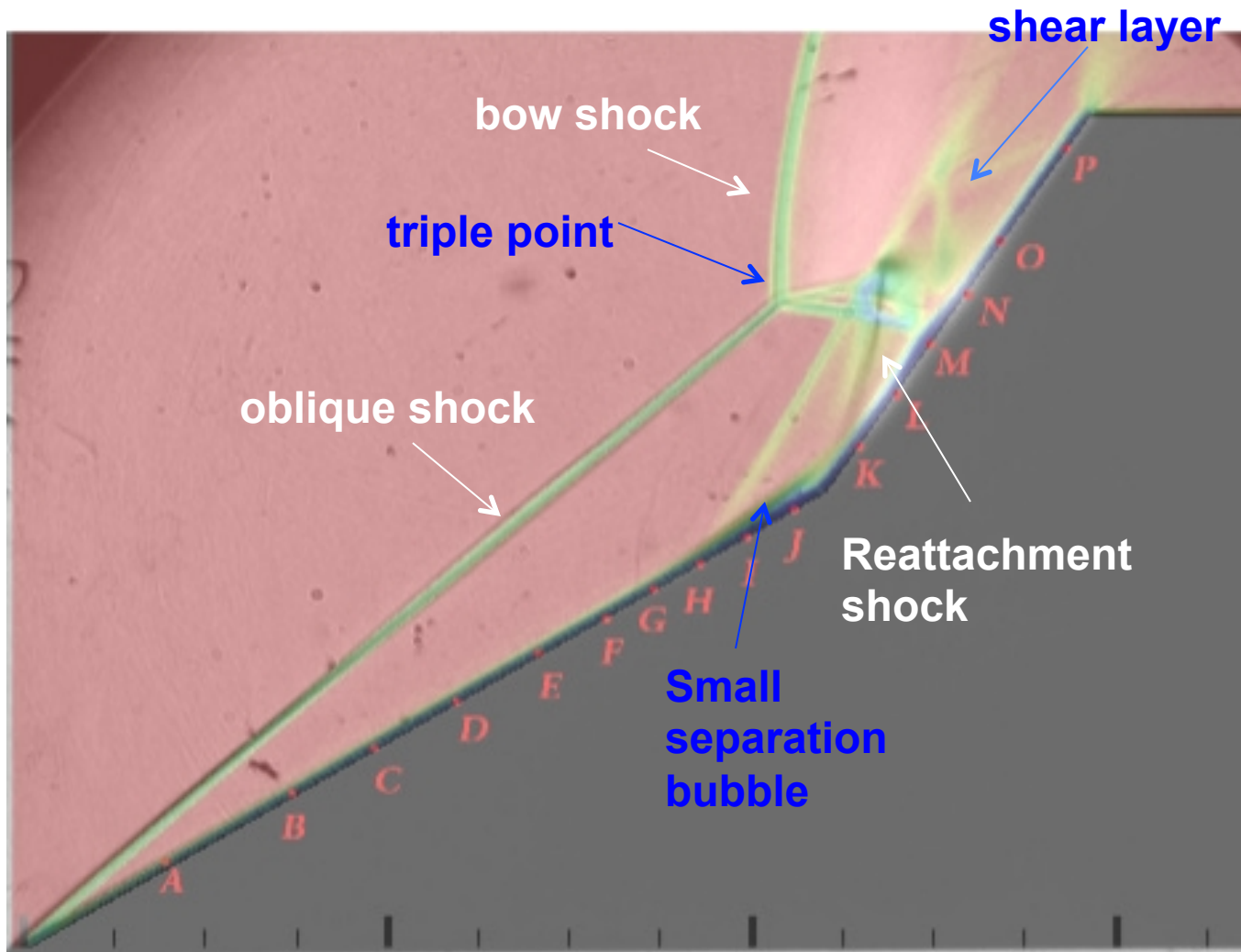
Strong Shock Interactions – High Enthalpy Case



- separation and reattachment shocks
- triple point
- shear layers
- boundary layer interactions
- attached shock from the first cone/wedge interacts with the detached bow shock from the second cone/wedge.

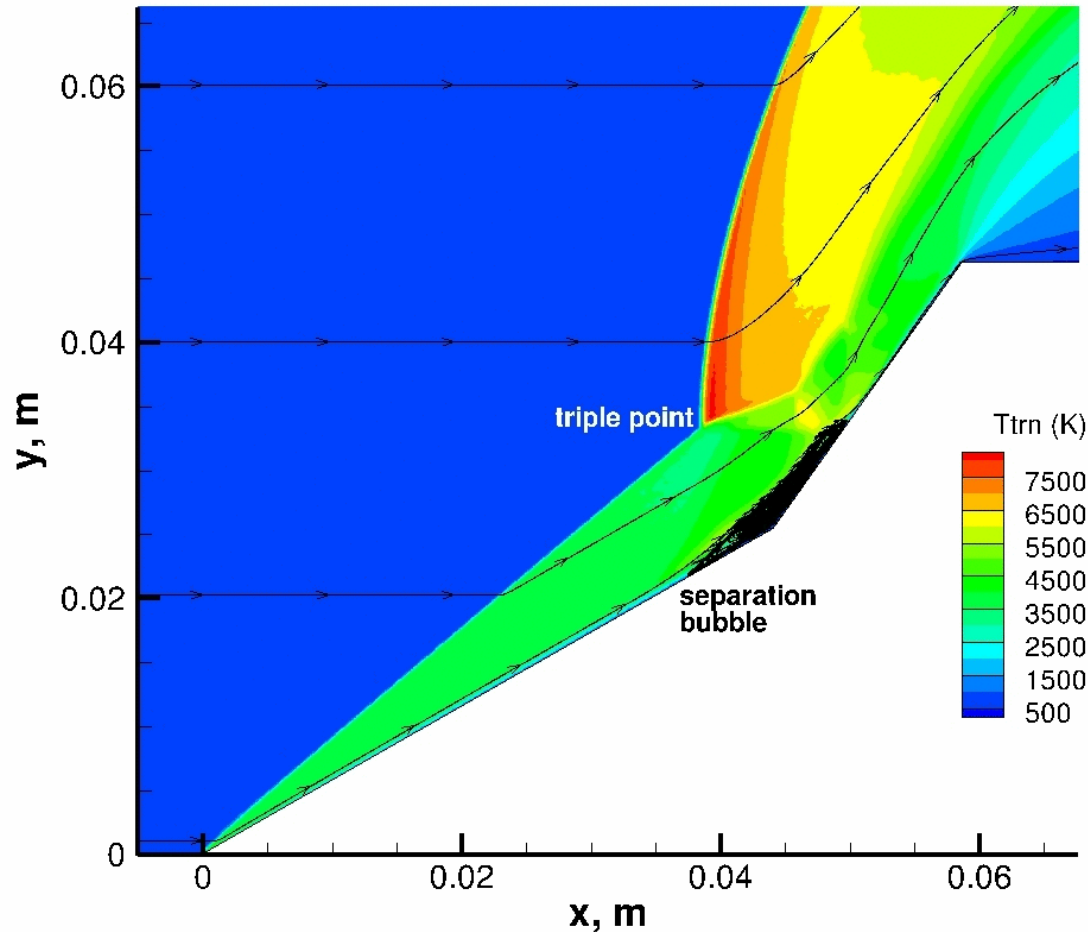


HE case : Schlieren Comparison



- **Overlap of Schlieren plot from DSMC result at 100,000 timesteps (100 μ s) with Schlieren Image from experimental data (test time is 242 μ s).**
- **Best agreement with the shock structure and the size of the separation region between the experimental and computational Schlieren images.**

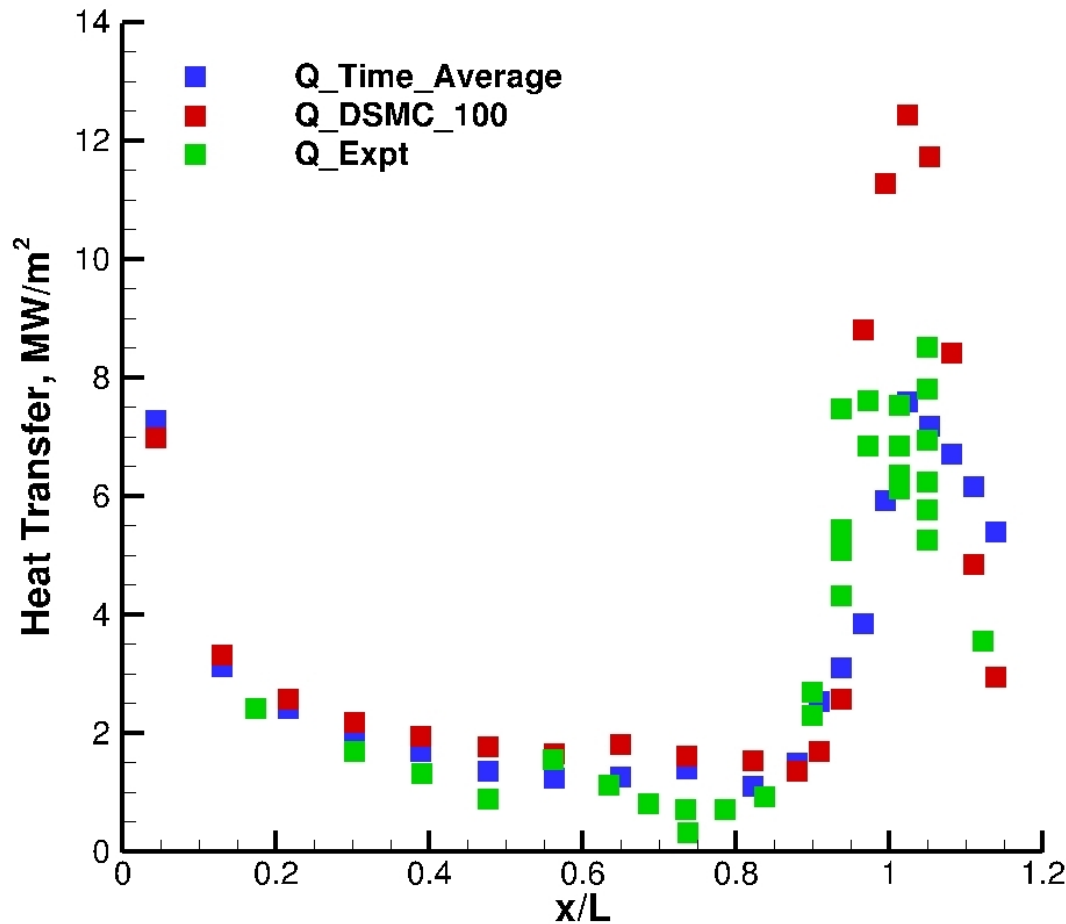
HE case : Time dependent solution



Translational Temperature Contour Plots
(70 μ s, 100 μ s, 160 μ s, 300 μ s)

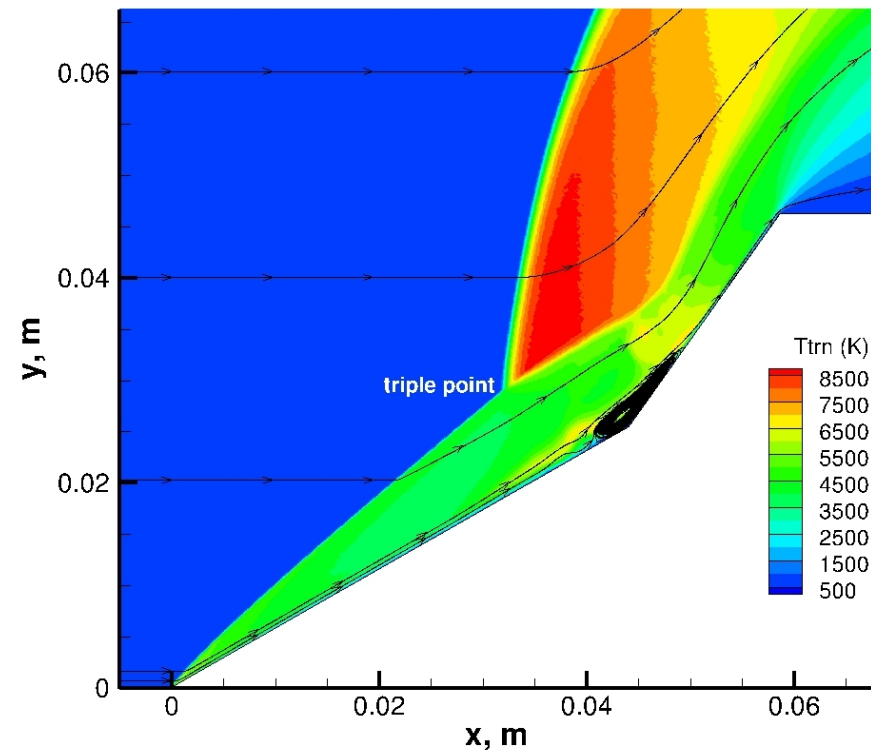
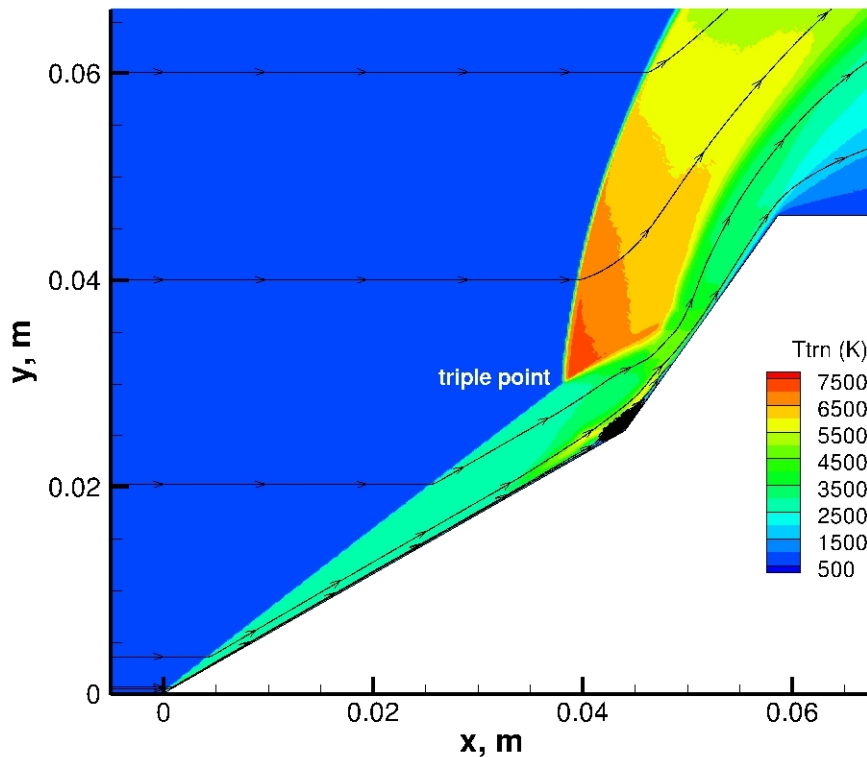
- The size of the separation bubble keeps on increasing.
- The triple point location starts to shift downstream.
- Separation shock moves ahead on the leading edge and interacts earlier with the oblique shock leading to new flow features.
- Flow is unsteady and does not attain a steady state.

HE case : Heat Transfer



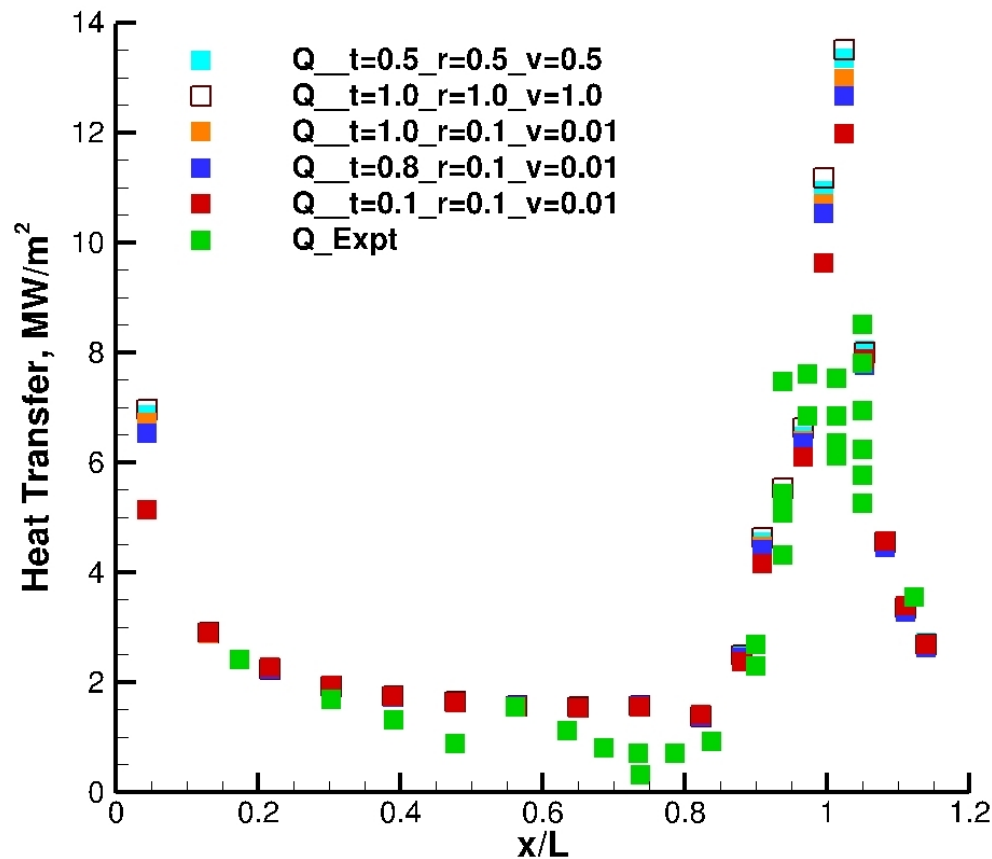
- The computational results show a similar trend to the experimental values and capture the jump at the hinge ($x/L = 0.8$).
- But the DSMC computations tend to over-predict the heat transfer rates in the area of shock impingement on the aft wedge.
- The weighted time average of heat transfer (from $100\mu\text{s}$ to $400\mu\text{s}$) brings the peak heat transfer into better agreement with the experiment.

HE case : R-T and V-T relaxation



- **Constant values for relaxation numbers: fast relaxation rate $Z_r = Z_v = 2$ and slow relaxation rate $Z_r = Z_v = 1000$.**
- **Temperature dependent rotational and vibrational relaxation numbers for previous cases were about 8-10 for Z_r and around 1200 for Z_v .**

HE case : Gas Surface Interactions

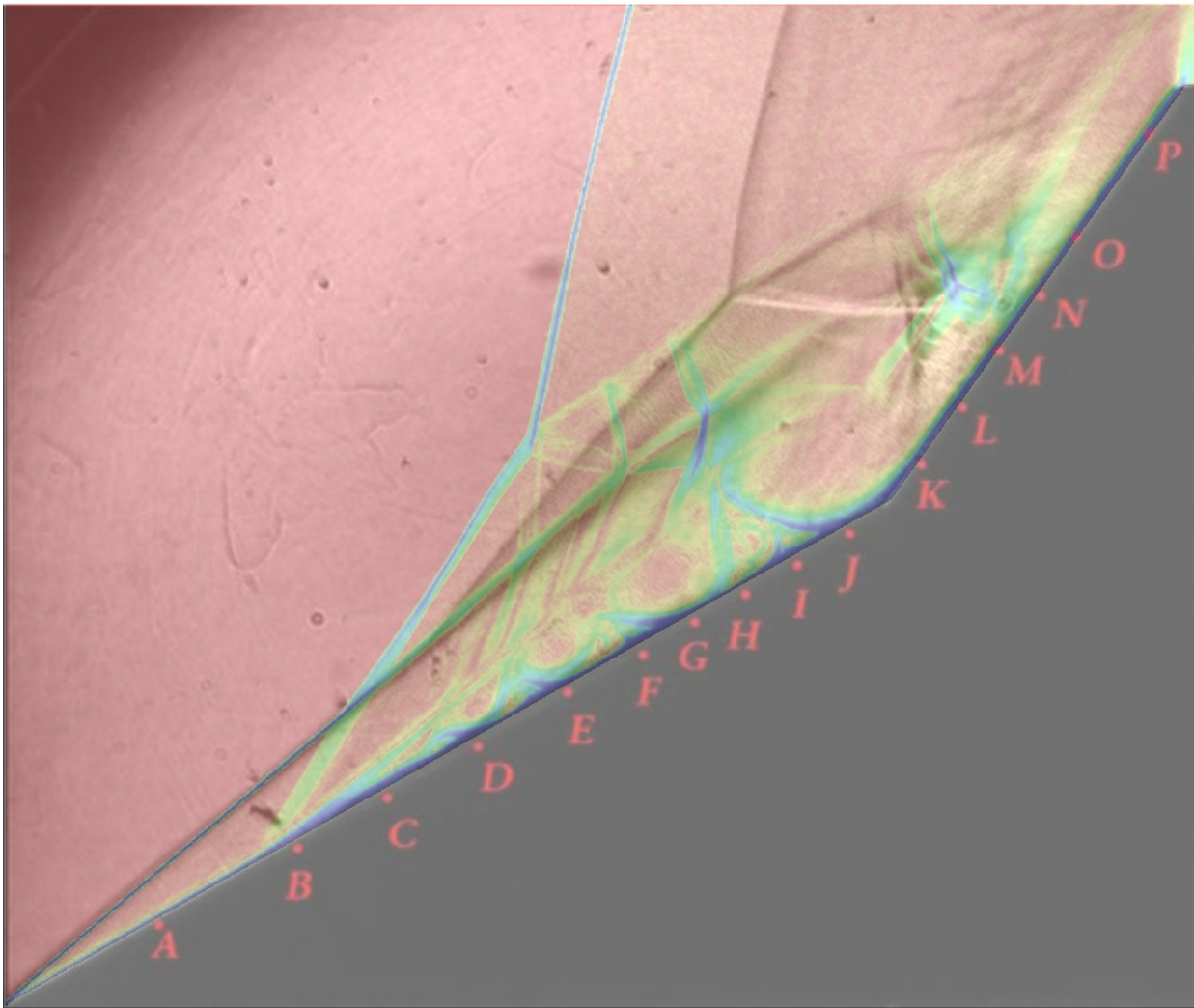


- Heat transfer rates are dependent on the gas - surface interaction model used.
- Thermal energy accommodation coefficients were varied.

| α_{trans} | α_{rot} | α_{vib} |
|------------------|----------------|----------------|
| 0.5 | 0.5 | 0.5 |
| 1.0 | 1.0 | 1.0 |
| 1.0 | 0.1 | 0.01 |
| 0.8 | 0.1 | 0.01 |
| 0.1 | 0.1 | 0.01 |

- It is reasonable to assume the following values for the surface energy accommodation coefficients, $\alpha_{trans} = 0.8$, $\alpha_{rot} = 0.1$, $\alpha_{vib} = 0.01$ based on the material used for the double wedge model experiment.

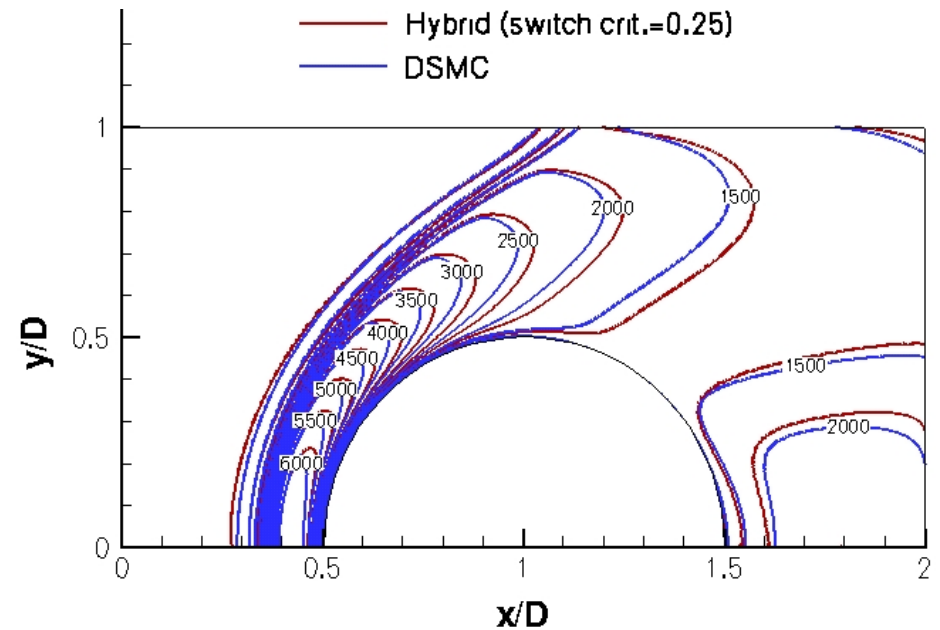
LE case : Schlieren comparison



- Superimposition of the predicted Schlieren at $320\mu\text{s}$ with the experimental image.
- Good agreement with the oblique shock and the size of the separation region.
- Different shock structure is observed near the second wedge.
- Triple point in experiment occurs at a higher y location as compared to the DSMC result, due to the difference in the interaction between the separation and oblique shocks.

Outstanding Scientific Issues

- To develop a basic computational framework based on the ellipsoidal statistical Bhatnagar-Gross-Krook (ES-BGK) model of the Boltzmann equation, capable of solving polyatomic multi-species gas flows.
- The new particle-based (Hybrid?) method should have the following features:
 - Be more efficient than DSMC in modeling high density flows,
 - Provide a transition to NS
 - Be sufficiently general to include internal energy
 - Apply to shock-shock interactions
- Start with flows where chemical reactions are not important.





Simplifications of Kinetic Equations

Boltzmann equation (spatially non-uniform case):

$$\frac{\partial}{\partial t}(nf) + \vec{v} \cdot \frac{\partial}{\partial \vec{r}}(nf) + \vec{F} \cdot \frac{\partial}{\partial \vec{v}}(nf) = \left[\frac{\partial}{\partial t}(nf) \right]_{\text{collisions}}$$

$$\left[\frac{\partial}{\partial t}(nf) \right]_{\text{collisions}} = \int_{-\infty}^{\infty} \int_0^{4\pi} n^2 (f^* f_1^* - ff_1) v_r \sigma d\Omega d\vec{v}$$

Thermal diffusion rate
Viscous diffusion rate

$$(Pr = C_p \mu / \kappa)$$

BGK collision model (much simpler):

$$\left[\frac{\partial}{\partial t}(nf) \right]_{\text{collisions}} = nv(f_e - f) \quad v = Pr \frac{nkT}{\mu}$$

Lacks accuracy

$$(Pr = 1.0)$$

ES-BGK collision model (still simple):

$$\left[\frac{\partial}{\partial t}(nf) \right]_{\text{collision}} = nv(f_{\text{ellipsoidal}} - f)$$

Corrects the *Pr* unity problem

A fraction of particles in a cell is randomly selected. New velocities are assigned from a Maxwellian/ES distribution function.

Solution of BGK/ES-BGK Equation by Statistical Method

- A fraction of particles in a cell randomly selected. New velocities according to the Maxwellian/ES distribution function assigned.
- The velocities of particles, not selected, remain unchanged.
- Internal modes are relaxed to equilibrium at appropriate rates.

- The relaxation frequency for rotational equilibrium:

$$\nu_R = \frac{F_{\text{coll}}}{Z_R}$$

- Rotational collision number: $Z_R = \frac{3/5 Z_R^\infty}{1 + (\pi^{1/2} / 2)(T^* / T_{\text{eq}})^{1/2} + (\pi + \pi^2 / 4)(T^* / T_{\text{eq}})}$

- Number of particles selected for relaxation:

$$N_C = N(1 - \exp(-\nu \Delta t))$$



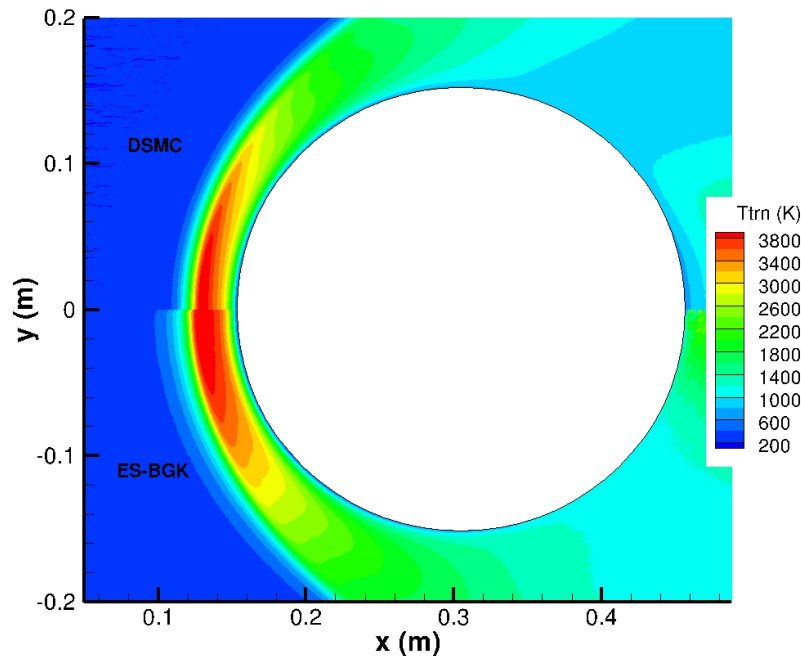
Two Simple Test Cases DSMC vs BGK

| Freestream Parameters | Case 1: High M | Case2: Low M |
|----------------------------|-----------------------|-----------------------|
| Sphere diameter (m) | 0.05 | 0.3048 |
| Mach number – M | 14.56 | 9.13 |
| Static Temperature (K) | 200 | 200 |
| Static Pressure (kPa) | 2.577 | 1.222 |
| Velocity (m/s) | 4200 | 2634.5 |
| Density (/m ³) | 4.34x10 ⁻⁴ | 2.06x10 ⁻⁵ |
| Knudsen number | 1.28x10 ⁻³ | 8.9x10 ⁻³ |

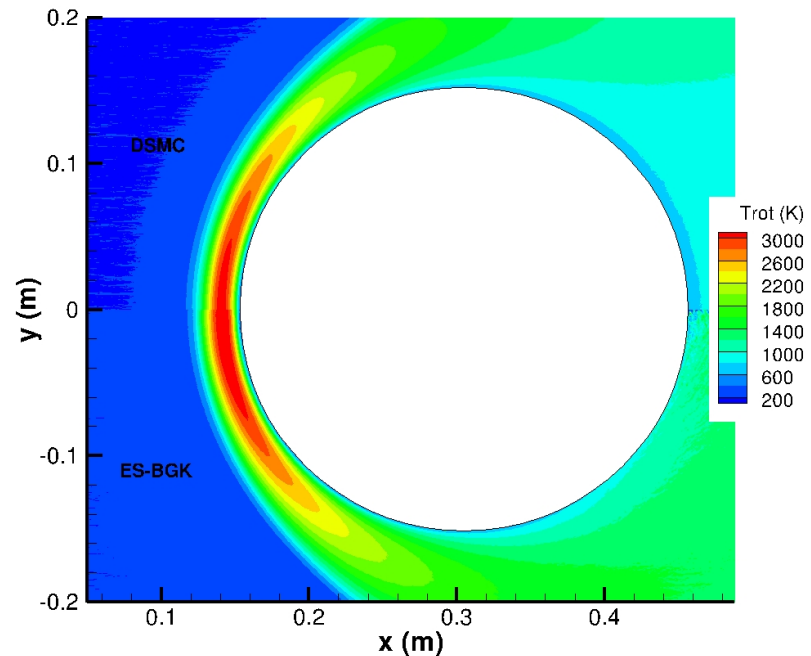


Case II Mach 9: Comparison of Temperature Contours: *In Progress*

Translational Temperatures

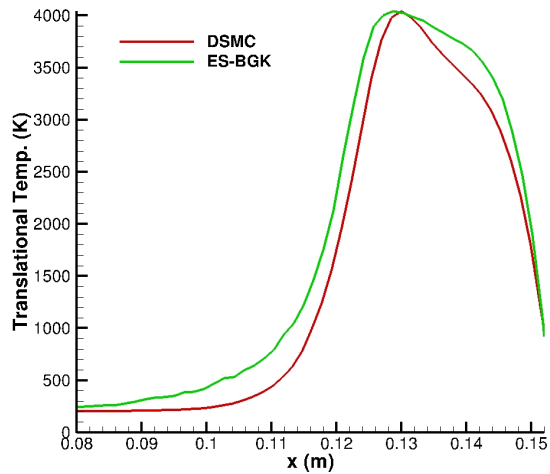


Rotational Temperatures

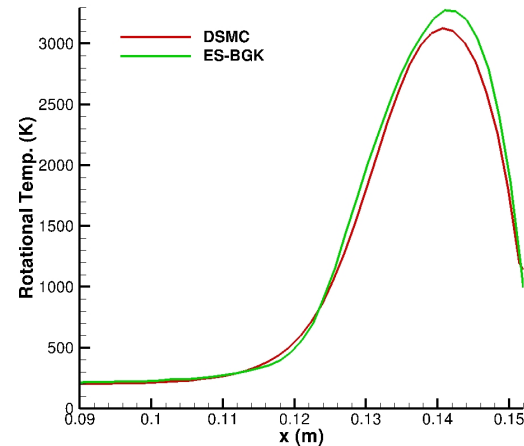


- Translational temperature profiles are similar, but thickness of the shock is wider in ES vs. DSMC.
- The width of the DSMC shock is about 0.015 m while the ES-BGK shock width is around 0.02 m.
- Rotational temperatures are in better agreement

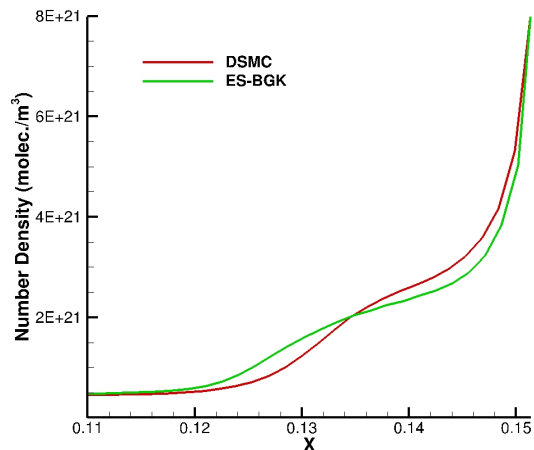
Case II : Stagnation Line Profiles: *In Progress*



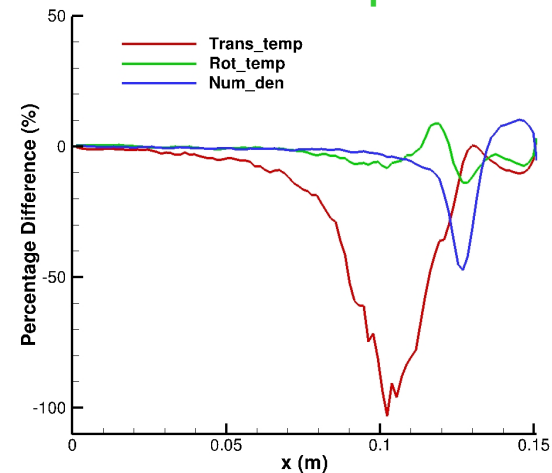
Translational temperature



Rotational temperature



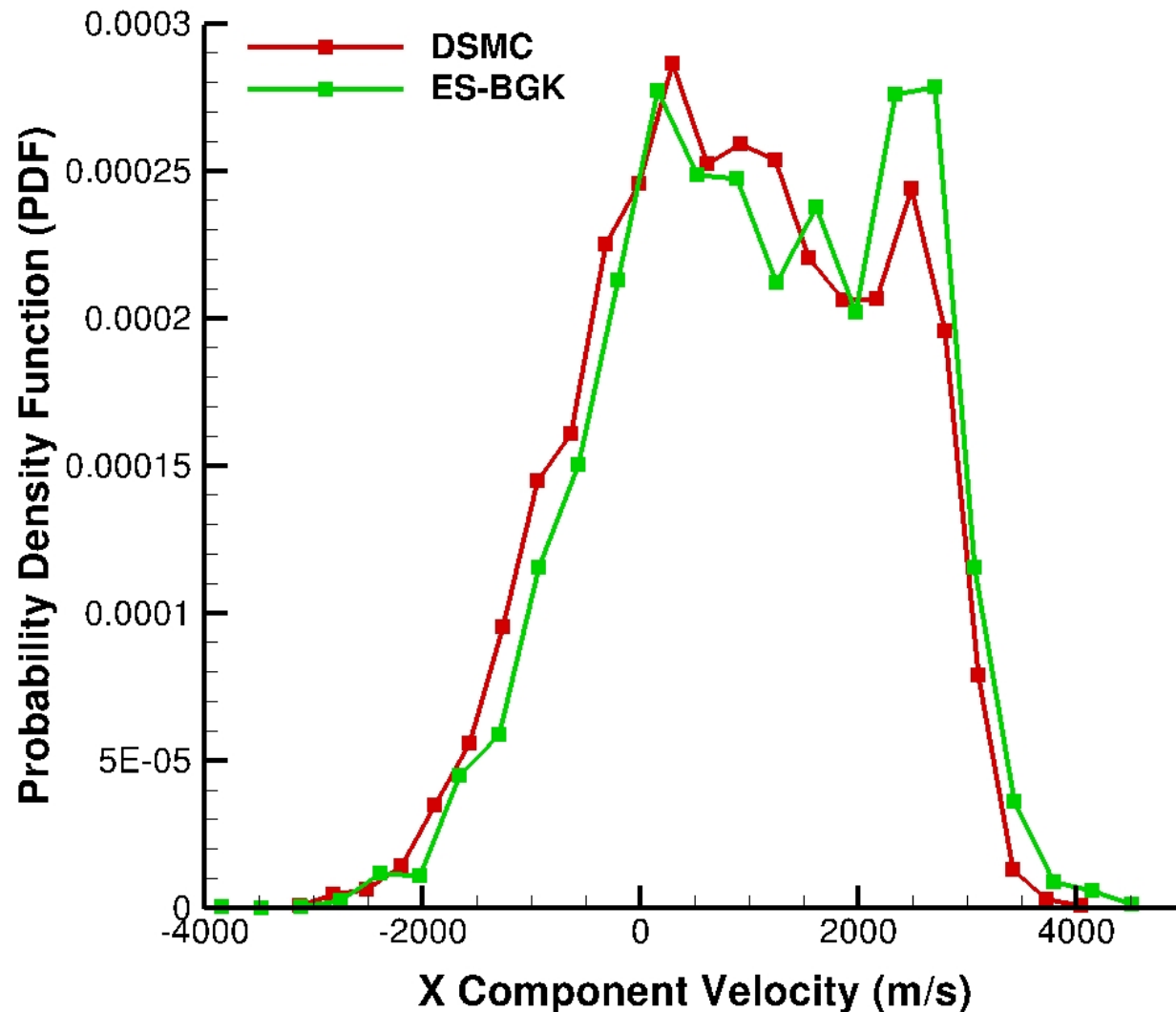
Number density



Percentage difference

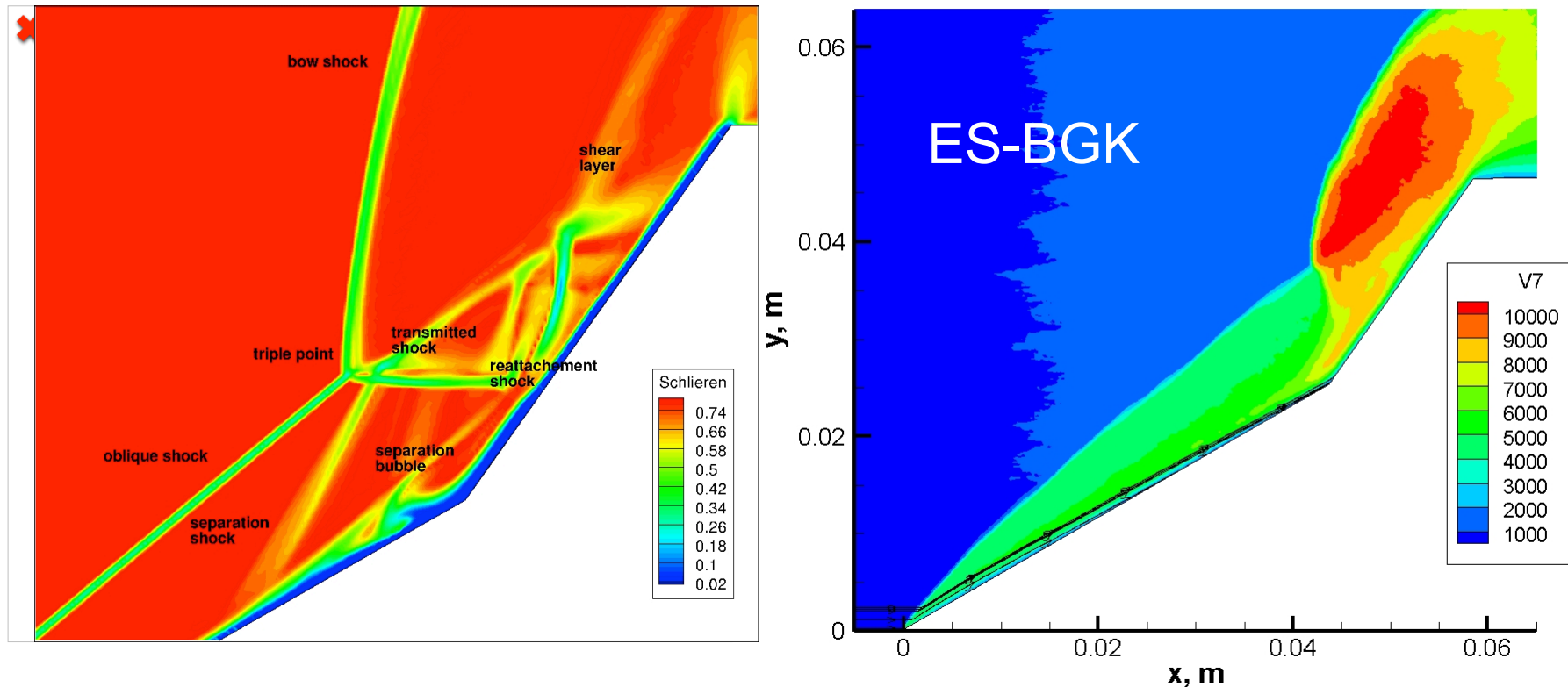
- Difference in DSMC vs ES-BGK number density and rotational temperatures are small.
- But the translational temperature shows considerable deviation, due to the difference in the shock width.

Case II : Velocity PDF inside Shock



- Departure from Maxwellian distribution is seen at $x=0.13$ (for DSMC) and $x=0.125$ (for ES-BGK), in the center of the shock.
- Both ES-BGK and DSMC predict the bi-modal nature of the x-component velocity distribution.

Comparison of DSMC vs BGK Shock-Shock Interactions



- DSMC resolves experimentally observed complex shock structures,
- In BGK, an oblique shock, bow shock, and triple point can be seen, but, there is no separation region. Why not?



Outstanding Scientific Issues

- **Our fundamental understanding of laminar shock-shock interactions is far from complete:**
 - Essentially no chemistry, single species,
 - Eliminates many uncertainties in physical models.
- **Top priorities are the investigation of 3-D vs 2-D effects on the unsteadiness of the DSMC modeled flows.**
- **This data set is part of the AVT-205 so that comparisons with NS/CFD will be interesting.**
- **Development of particle-based algorithm, ES-BGK for compression and shock-shock interactions:**
 - progression from simple to hard, i.e., flow over a sphere, flow over a flat plate at variable AOA to get separation, and double wedge.
 - is there a breakdown criteria?
 - will ES-BGK provide a bridge between DSMC and NS?
 - is it computationally worth it compared to promise of new AMR grid techniques?
- ***Future transitions: modeling of NO formation.***



Acknowledgments

Research performed at the Pennsylvania State University was supported by AFOSR Grant No. AFOSR Grant No. FA9550-11-1-0129 with a subcontract award number 2010-06171-01 to PSU. We are very grateful to Prof. Austin of the University of Illinois for her helpful advice and inputs during the course of this investigation.